Zootaxa 0000: 0–0000 (2011)
www.mapress.com/zootaxa/

Article

ISSN 1175-5326 (print edition)
ZOOTAXA
ISSN 1175-5334 (online edition)

A reappraisal of the monophyly of the genus *Pseudomonocelis* Meixner, 1943 (Platyhelminthes: Proseriata), with the description of a new species from the Mediterranean

MARCO CASU, PIERO COSSU, DARIA SANNA, TIZIANA LAI,
FABIO SCARPA & MARCO CURINI-GALLETTI[1]

Dipartimento di Zoologia e Genetica Evoluzionistica, Università di Sassari, Via F. Muroni 25, 07100 Sassari, Italy. Centro di Eccellenza dell'Università di Sassari

[1]Corresponding author. E-mail: curini@uniss.it

Abstract

Pseudomonocelis paupercula **nov. sp.** is described from brackish-water habitats of the Mediterranean. It is distinguished from other members of the genus by the copulatory organ provided with a stylet, combined with lack of vagina and presence of a muscular organ close to the female pore. Its phylogenetic relationships have been investigated sequencing complete 18S rRNA gene and partial 28S rRNA gene, spanning variable domains D1-D6. Both BI and ML suggest a sister-taxon relationships of *P. paupercula* **nov. sp.** with the east African *P.* cf *cavernicola.* However, statistical support is low. Conversely, MP indicates *P. paupercula* **nov. sp.** as sister-taxon to all the remaining *Pseudomonocelis* and *Minona ilenae*. Overall, results of the combined analysis do not support the monophyly of the genus *Pseudomonocelis*. The need for wider molecular and taxonomic sampling is stressed.

Key words: *Pseudomonocelis paupercula*, microturbellarian, karyotype, taxonomy, biodiversity, molecular phylogeny, 18S, lrsDNA

Introduction

The Monocelididae Hofsten, 1907 (Platyhelminthes: Proseriata) include marine interstitial flatworms, with a comparatively simple morphology. Among the few morphological characters on which their systematics is based, particular weight has been traditionally attributed to the position of the ovaries in relation to the pharynx (Martens, 1983). In most Monocelididae the ovaries are placed just in front of the pharynx, while a few species display post-pharyngeal ovaries. However, the paucity of characters available for taxonomy and the chances of parallel evolution raise suspicions that groupings of taxa exclusively based on relative position of the ovaries may be homoplastic (Martens, 1983; Curini-Galletti *et al.*, 2010). Among the genera with posterior ovaries, the genus *Pseudomonocelis* Meixner, 1943 appears indeed particularly heterogeneous. It includes species showing all stages from the presence of a fully functional accessory organ provided with a stylet (*Pseudomonocelis hoplites* Curini-Galletti, 1997) to a reduced state which has lost both the stylet and the glandular function (*P. cavernicola* Schockaert & Martens, 1987), to the total loss of the organ (Curini-Galletti, 1997; Curini-Galletti & Casu, 2005; Curini-Galletti *et al.*, 2011; Schockaert & Martens, 1987). So far, the monophyly of the genus has never been tested using gene sequence data. *Pseudomonocelis hoplites* has not been sequenced yet. *Pseudomonocelis* cf *cavernicola*, in a molecular study of the *Pseudomonocelis agilis* complex, clustered with the rest of the *Pseudomonocelis* species (Casu *et al.*, 2009). However, branch support was very low, and the molecular sample too limited to allow any sound conclusions.

Recently, during sampling campaigns performed in the Mediterranean under the sponsorship of the project BIOIMPA ('Biodiversity of Inconspicuous Organisms in Marine Protected Areas'), a new species of *Pseudomonocelis* was found which, similarly to *P.* cf *cavernicola*, presents an accessory organ without stylet. Here we present

Accepted by W. Sterrer: 23 Jul. 2011; published: ?? Month 2011

the description of this species, as well as new insights on the phylogenetic relationships of the species currently attributed to the genus *Pseudomonocelis*.

Material and methods

Sampling and karyological analysis. The specimens were found in samples collected manually from the following localities: Porto Pozzo, Sardinia, Italy (PP); Maliakós, Greece (MA); Alexandria, Egypt (AL) and Akko, Israel (AK) (see species description for further information on the stations). In all instances, the sediment consisted of silty sand. Extraction of the animals was through the $MgCl_2$ decantation technique (Martens, 1984), modified according to the quantity of silt in the sediment. After about 10 min immersion in a $MgCl_2$ solution isotonic to sea water, the sediment was stirred, and the suspension filtered through comparatively coarse sieves of decreasing mesh size (300 µm to 140 µm). The sieves were rinsed with sea-water in Petri dishes till silt was washed away. They were then placed to rest, until the animals crawled across the sieves in the Petri dish, and were retrieved with the aid of a stereomicroscope.

Whole mounts were done with polyvinyl-lactophenol. For microscopical analysis material was fixed in Bouin's fluid, embedded in 60º C Paraplast and cut into serial sagittal sections at 4 µm, stained with Hansen's haematoxylin and eosin-orange and mounted in Eukitt. For molecular analysis, specimens were fixed in 95% ethanol and stored at 4° C until DNA extraction.

Karyotype was determined from acetic-orcein-stained spermatogonial mitoses as described by Curini-Galletti *et al.* (1985). Relative lengths (r.l. = length of chromosome × 100/total length of haploid genome), centrometric indices (c.i. = length of short arm × 100/length of entire chromosome) and haploid genome length (g.l.) were obtained from measurements of camera lucida drawings of metaphase plates. The fundamental number (F.N.) is derived according to Matthey (1949) and chromosome nomenclature follows Levan *et al.* (1964).

Comparisons among karyotypes were based on plates obtained from 10 specimens per population. From each specimen, one plate, showing average contraction, was measured. Unifactorial ANOVA was performed on seven karyological variables. 'Population' factor was treated as fixed. Interpopulational differences were deemed as significant with $P \leq 0.01$. Cochran's *C*-test was used to test assumption of homogeneity of variances.

The holotype is deposited in the collections of the Swedish Museum of Natural History (Stockholm, Sweden) (SMNH). Paratypes and additional material are deposited in the collection of the Zoological Museum of the University of Sassari (Italy) (CZM).

Molecular analysis. Genomic DNA was extracted using the QIAGEN DNeasy Tissue kit (QIAGEN Inc.) according to the supplier's instructions. After extraction, the DNA was stored as a solution at 4 °C.

Six individuals belonging to each population were sequenced at complete nuclear small subunit rRNA (18S) gene, and partial nuclear large subunit rRNA (28S) fragment, spanning variable domains D1-D6 (see Table 1 for GenBank Accession numbers). Amplifications for both regions were carried out using the following external primers (see Littlewood *et al.*, 2000): for 18S: A (forward) AMC TGG TGG ATC CTG CCA G, and B* (reverse) TGA TCC ATC TGC AGG TTC ACC T; for 28S: LSU5 (forward) TAG GTC GAC CCG CTG AAY TTA AGC A, and LSUD6-3* (reverse) GGA ACC CTT CTC CAC TTC AGT C.

The polymerase chain reaction (PCR), carried out in a total volume of 25 µl, contained 5 ng/µl of total genomic DNA on average, 2.5 U of Taq DNA Polymerase (Euroclone), 1× reaction buffer, 1.25 mM of $MgCl_2$, 0.4 µM of primers, and 200 µM of dNTPs. PCR amplification was carried out in a MJ PTC-100 Thermal Cycler (MJ research) programmed as follows: 1 cycle of 3 min at 94° C, 45 cycles of 40 s at 94° C, 45 s at 54° C (18S / 28S D1-D6 primers' annealing temperature), and 1 min and 40 s at 72° C. At the end, a post-treatment for 5 min at 72° C and a final cooling at 4° C were carried out. Both positive and negative controls were used to test the effectiveness of the PCR reagents.

Electrophoresis was carried out on 2% agarose gels, prepared using 0.5× Tris-Borate-EDTA buffer, at 4 V/cm for 20 min and stained with ethidium bromide (10 mg/ml). PCR products, purified by ExoSAP-IT (USB Corporation, under license from GE Healthcare) following the manufacturer's instructions, were sequenced for both forward and reverse 18S and 28S D1-D6 strands, using an external sequencing core service (Macrogen Inc., Korea).

We also sequenced for both 18S and 28S D1-D6 one individual belonging to each of the monocelidid species listed in Table 1. Taxonomic information and full geographical data for these species are given in Casu *et al.*, 2009,

2011; Curini-Galletti & Casu, 2005; Curini-Galletti *et al.*, 2011; Lai *et al.*, 2008.

Sequences of the outgroup *Archimonocelis staresoi* Martens & Curini-Galletti, 1993 (Proseriata: Archimonocelididae) were those of Littlewood *et al.* (2000). No further species belonging to Monocelidinae were added to the dataset, since published sequences of both fragments were not available.

TABLE 1. List of species sampled and sequences used for this study. Accession numbers refer to GenBank codes; accession numbers of new sequences are in bold.

Species	Locality	SSU	LSU D1-D6
Pseudomonocelis paupercula **nov. sp.**	see text	JN224901-904	JN224915-918
Pseudomonocelis ophiocephala (Schmidt, 1861)	Porto Torres (Sardinia, Italy)	JN224895	JN224907
Pseudomonocelis agilis (Schultze, 1851)	Helsingør (Denmark)	JN224897	JN224912
Pseudomonocelis cf *cavernicola* Schockaert & Martens, 1987	Dongwe (Zanzibar)	JN224900	JN224914
Pseudomonocelis cetinae Meixner, 1943	Omiš (Croatia)	JN224899	JN224913
Pseudomonocelis occidentalis Curini-Galletti, Casu & Lai, 2011	Porto Pozzo (Sardinia, Italy)	JN224894	JN224909
Pseudomonocelis orientalis Curini-Galletti, Casu & Lai, 2011	Maliakós (Greece)	JN224896	JN224908
Minona ileanae Curini-Galletti, 1997	Great Bitter Lake (Egypt)	JN224905	JN224910
Monocelis lineata (Müller, 1773)	Ferrol (Galicia, Spain)	JN224906	JN224911
Archimonocelis staresoi Martens & Curini-Galletti, 1993	Porto Cesareo (Lecce, Italy)	AJ270152	AJ270166

The 18S and 28S D1-D6 sequences were aligned using Clustal W (Thompson *et al.*, 1994), implemented in BioEdit 7.0.5.2 software (Hall, 1999).

The best probabilistic model of sequence evolution was determined for 18S and 28S D1-D6 after evaluation by JModeltest 0.1 (Posada, 2008) with a maximum likelihood optimised search, using the Akaike Information Criterion (AIC). The model GTR+G for both 18S and 28S D1-D6 has been calculated as the best fitting.

Phylogenetic relationships among individuals and species were investigated using the Bayesian Inference (BI), the Maximum Likelihood (ML) and the Maximum Parsimony (MP), using the combined dataset of 18S and 28S D1-D6.

The software MrBayes 3.1.2 (Ronquist & Huelsenbeck, 2003) was employed for the BI, specifying a partitioned model and settings N_{ST} = 6, rates = gamma, ngammacat = 4. Two independent runs each consisting of four Metropolis-coupled MCMC chains (one cold and three heated chains) were run simultaneously for 5,000,000 generations, sampling trees every 1,000 generations. We allowed each partition to have his own set of parameters and a potentially different overall evolutionary rate. The first 25% of sampled trees were discarded. Convergence of chains was checked following the procedures described by Huelsenbeck & Ronquist (2001) and by Gelman *et al.* (1995). Nodes with a percentage of posterior probability lower than 95% are considered not highly supported.

ML was obtained using the genetic algorithm implemented in GARLI 2.0 (Zwickl, 2006). In order to find the best tree the configuration file for partitioned models was set up to perform 10 replicate searches (searchreps = 10). Model parameters: ratematrix = (0 1 2 3 4 5), ratehetmodel = gamma, numratecats = 4, corresponding to the evolution model suggested by JModeltest (GTR+G) for both 18S and 28S D1-D6 were used. In order to allow independent estimates of the parameters for each gene the option link was set to 0. In addition, since we have two models, Modweight was set to 0.0015. Finally, node support was assessed by 1000 bootstraps (bootstrapreps = 1000).

For MP (software PAUP*, Swofford, 2003), heuristic analyses with tree-bisection-reconnection (TBR) branch-swapping were used with 100 iterations each beginning with random starting trees. MP bootstrap support was assessed with 1000 bootstrap iterations (full TBR heuristic searches). For ML and MP, nodes with a percentage of bootstrap lower than 50% are considered not highly supported.

Results

Taxonomy

Family Monocelididae Hofsten, 1907

Genus *Pseudomonocelis* Meixner, 1943

Pseudomonocelis paupercula Curini-Galletti, Casu & Lai nov. sp.

(Figs 1, 2)

Material. Holotype: Italy, Sardinia, Porto Pozzo (41°11'20.22"N; 9°17'11.03"E), lower intertidal in brackish water; very silty mixed sand (May 2004); sagittally-sectioned (SMNH Type-8082). Paratypes: three specimens sagittally-sectioned (CZM 408 - 410); two whole mounts (in one slide) (CZM 411), same data as holotype. Additional material from the type locality: 10 specimens for karyology.

Greece, Gulf of Maliakòs, near Stylida (38°54'26.05"N; 22°37'22.25"E), lower intertidal in mixed, silty sand, near a fresh-water outlet (March 2004). 11 specimens, sagittally sectioned (CZM 412 - 422); 10 specimens for karyology.

Israel, Akko, Western Wall (32°55'29.94"N; 35°4'5.55"E), mixed sediment in rocky pools (October 1997). 10 specimens, sagittally sectioned (CZM 423 - 432); two specimens used for karyology.

Egypt, Alexandria, Montazah Palace (31°17'16.68" N; 30°0'35.16"E) mixed sediment at the mouth of a fresh-water outlet (October 2003). 15 specimens, sagittally sectioned) (CZM 433 - 447); 10 specimens for karyology.

Etymology. From lat. *pauper* poor. Named for the small and poorly visible copulatory organ, the unusually small chromosomes for the genus, and its overall, non-descript appearance.

Note. The authorship of the species is limited to the three authors who most effectively contributed to the species description.

Diagnosis. Unpigmented *Pseudomonocelis* with copulatory organ provided with a stylet 15-29 µm long. With swollen female duct, and an unarmed accessory organ close to the female pore.

Description. Fixed mature specimens up to 2.8 mm long (holotype: 2.5 mm; paratype: 2.2 mm), elongate and cylindrical (Fig. 1A). Living animals appear opaque due to gut content and internal organs, especially vitellaria. Without pigmented eyespots. Epithelium with insunk nuclei, ciliated. Cilia about 2.5 µm long ventrally, 2 µm dorsally. Ventral side entirely ciliated, apart from the area surrounding the female pore. Dorsally, the caudalmost area is unciliated. Frontal end with oily droplets. Ovoid rhabdoids 11-15 µm in length. 10-12 rhabdoid glands, particularly large and conspicuous, and easily noticeable in living specimens (Figs 1A, 2E), are present caudally. These glands lie deeply imbedded in the parenchyma (Figs 1D, 2D). Adhesive glands arranged radially at the posterior tip of the body. Animals can quickly modify the shape of the tail, from narrowly elongate to spatulate, and adhere strongly to the substrate.

Statocyst about 25 µm in diameter; containing one statolith about 15 µm long. The ovoid brain, 55 µm long and 50 µm wide in the holotype, abuts the statocyst. Body musculature formed by a very thin outer circular layer, and a thicker inner longitudinal layer. With a few transverse muscular fibres. Pharynx in mid-body, comparatively small, 150-200 µm long in mature specimens. Internally, it is ciliated in its distal half, with cilia 3-3.5 µm long; externally, it is uniformly ciliated (cilia 1–1.5 µm long), apart from the distal tip, where pharyngeal glands discharge. With a well developed oesophagus, about half the length of the pharynx. Musculature of pharynx inverted with respects to body musculature. The inner circular component is particularly strong distally, while it is not present below the oesophagus. Pharyngeal glands well developed, extending anteriorly in the body, and easily seen in living, squeezed specimens.

Male genital organs. With very few (5–10), ventral testes. Copulatory organ of the simplex-type (see Litvaitis *et al.*, 1996), placed close to the ovaries. In some large, otherwise mature animals the copulatory organ is totally lacking (CZM 412, 422, 436, 439) or presumably non functional (CZM 435, 440). The copulatory organ is formed by a seminal vesicle lined by a muscular sheath and a penis papilla provided with a stylet (Fig. 1C). Shape and size of the bulb strongly depend on contraction during fixation and amount of sperm content. It is 87 µm high, 81 µm wide in the holotype (Fig. 2C); much smaller and regularly spherical (32 µm across) in the paratype, where sperm was not present. The bulb of specimens from Akko ranged from 40 µm high and 35 µm wide to 105 µm high and

93 µm wide. In specimens from Maliakos, the bulb ranged 28–40 µm high, and 34–53 µm wide (Figs 2A, B). In specimens from Alexandria it ranged 24–43 µm and 20–64 µm respectively. The bulb is lined by an outer layer of circular musculature, and an inner layer of longitudinal musculature. The thickness of the muscular wall depends on its state of contraction. It is about 2 µm thick in the holotype, and ranges from up to 7.5 µm in specimens with a small, contracted bulb to less than 1 µm in diameter in the largest bulbs of specimens from Akko. The seminal vesicle is lined by a thin epithelium, which becomes high and glandular distally, where it is pierced by the outlet of prostatic glands, whose nuclei lie outside the bulb. The prostatic glands are few, and poorly developed. The penis papilla is small and conical, and is formed mostly by circular musculature. It is provided with a copulatory stylet. The stylet is pen nib-shaped, with a broader basis and a distal, gutter shaped pointed tip. The stylet is 26 µm long in the holotype (Fig. 2C), and ranged 15–29 µm in the sample. The stylet is wrapped by the penis papilla, and its basis may protrude into the bulb. It has been observed in all the sectioned specimens from the type locality, which were large, mature animals. In the other populations, it has been detected in most specimens; it was absent in few specimens only, with the smallest copulatory bulbs. The stylet is thus presumably formed at full male maturity. Nonetheless, due to its small size and poor sclerification, the stylet can be detected in mature living specimens with great difficulty. On the contrary, it is easily noticeable in sectioned specimens, as it is intensely eosinophilous. The male antrum is small and unciliated, and opens to the outside through the male pore.

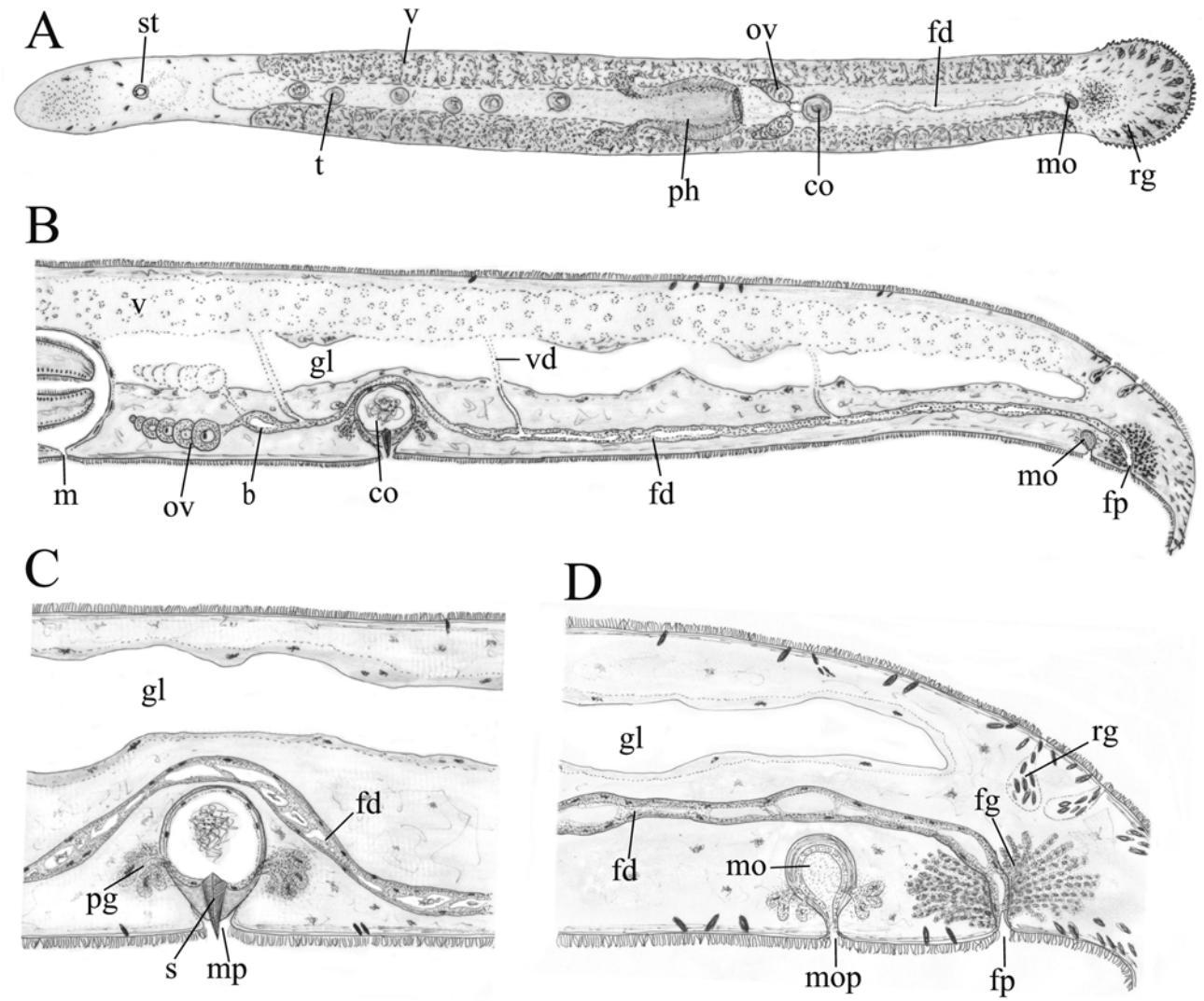

FIGURE 1. *Pseudomonocelis paupercula* **nov. sp.** A: general appearance; B–D: sagittal reconstructions of the post-pharyngeal regions (B), copulatory organ (C); female genital organ and muscular organ (D). Abbreviations: b: bursa; co: copulatory organ; fd: female duct; fg: female glands; fp: female pore; gl: gut lumen; m: mouth; mo: muscular organ; mop: muscular organ pore; mp: male pore; ov: ovaria; pg: prostatic glands; ph: pharynx; rg: rhabdoid glands; s: stylet; st: statocyst; t: testes; v: vitellaria; vd: vitelloduct.

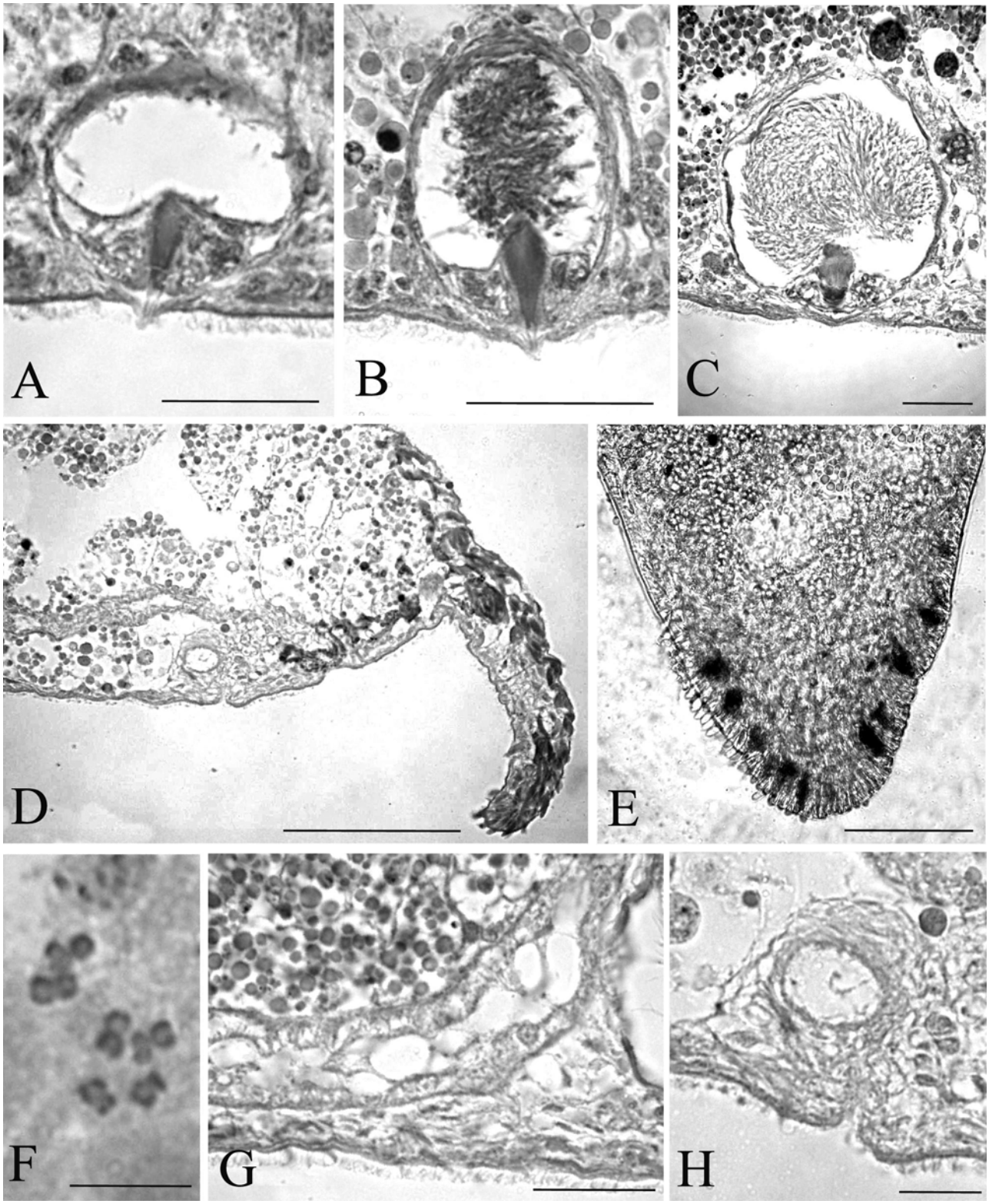

FIGURE 2. *Pseudomonocelis paupercula* **nov. sp.** A–C: sagittal sections of copulatory organs (A: CZM 413; B: CZM 414; C: SMNH Type-8082); D: sagittal section of the caudal area (CZM 408); E: caudal tip of a living specimen, showing the radial arrangement of rhabdoid glands; F: spermatogonial plate; G: detail of the female duct (SMNH Type-8082); H: detail of the muscular organ (CZM 408). Scale bar: A–C: 25 µm; D: 50 µm; E: 100 µm; F: 5 µm; G,H: 10 µm.

Female genital organs. With large, thick vitellaria, extending from behind the brain till the level of the copulatory organ. They are easily visible, due to their development, in living slightly squeezed specimens (Fig. 1A). Ovaria post-pharyngeal. Up to 15 oocytes per ovary are discernible in sections, the largest (up to 33 µm in diame-

ter) being the caudalmost. Shortly behind the ovaria, the two oviducts fuse into the female duct, which runs posteriorly and ventrally over the copulatory organ and opens to the outside through the female pore, just in front of the caudal end of the body (Fig. 1B). At the joining of the two oviducts, a few specimens show a widening, up to about 20 µm across, which may be interpreted as a small bursa (Fig. 1B). The entire female duct system is irregularly swollen along its course and is lined by a high, vacuolar epithelium (Fig. 2G). The development of vacuoles is to such an extent that the entire female duct, in sections, appears as lacking a continuous lumen. This peculiar lining extends to the oviducts, which are surrounded by vacuoles. Duct and vacuoles are often filled with sperm. Vitelloducts consisting of several, independent ducts (Fig. 1B). In some specimens, up to four vitelloducts could be traced, scattered along the length of the female duct, presumably connected to the overlying portion of the vitellaria. The most anterior vitelloducts join the oviducts, and are presumably connected to prepharyngean vitellaria. The female pore is surrounded by large, and numerous female glands (Fig. 1D).

Accessory organ. It is an ovoid, muscular organ, 14-17 µm wide, 16-25 µm high, located just in front of the female pore (Figs 1D, 2H). It is lined with a muscular sheath 2-2.5 µm thick, consisting mostly of longitudinal fibres, which are pierced by ducts of numerous glands, whose cell body lies outside the organ. The organ appears filled with the granular content produced by these glands, and opens to the outside through a short, narrow duct, very close to the female pore. Due to the reduced size of the organ, it is extremely difficult to discern in living specimens. In sections, it is easily detectable in large mature specimens only, and is absent in subadult specimens.

Karyotype. All populations showed karyotypes with haploid number n = 3, and F.N. = 6 (Fig. 2F). Chromosomes small and slightly differing in size: Chromosome 3 is about 75% of the length of Chromosome 1. Chromosomes 1 and 2 are metacentric; Chromosome 3 is submetacentric, with high index value. Karyometrical data of the populations used for statistical analysis (PP, MA, AL) are reported in Table 2. A unifactorial ANOVA based on the relative length and centromeric index of each chromosome and the haploid genome length was not significant, for any variable, at $P \leq 0.01$ (Table 2). Karyometrical data from two specimens from Akko closely corresponded to the other populations: Chrom. I = r.l.: 38.24 ± 3.32; c.i.: 46.33 ± 0.59; Chrom. II = r.l.: 32.45 ± 1.99; c.i.: 45.85 ± 1.45; Chrom. III = r.l.: 28.93 ± 5.74; c.i.: 35.65 ± 0.07; l.a.: 7.2 ± 0.8 µm.

TABLE 2. Karyometrical data (means ± SD) and results of the analysis of variance of three populations of *Pseudomonocelis paupercula* **nov. sp.**

		PP	MA	AL	$F_{(2,27)}$	P	
Chromosome 1	r.l.	38.15 ± 0.48	39.13 ± 0.45	38.61 ± 0.48	2.58	0.0944	n.s.
	c.i.	46.33 ± 0.65	47.18 ± 0.44	46.43 ± 0.27	0.93	0.408	n.s.
Chromosome 2	r.l.	32.96 ± 0.34	33.84 ± 0.22	32.43 ± 0.44	2.5	0.1009	n.s.
	c.i.	45.73 ± 0.53	46.41 ± 0.35	46.32 ± 0.49	0.64	0.5349	n.s.
Chromosome 3	r.l.	28.89 ± 0.69	27.03 ± 0.56	28.96 ± 0.84	3.95	0.031	n.s.
	c.i.	35.79 ± 1.13	35.61 ± 0.70	35.15 ± 0.93	0.12	0.884	n.s.
Haploid genome length (in µm)		7.5 ± 0.3	7.1 ± 0.2	7.2 ± 0.2	0.78	0.4682	n.s.

Molecular phylogenetic analysis

Sequences of 1672, and 1566 *bp* were obtained for 18S and 28S D1-D6 regions, respectively.

No sequence variation at both regions in any of the studied specimens was found. Therefore, in the trees (Figs 3-4), individuals of the same population have been joined into one terminal.

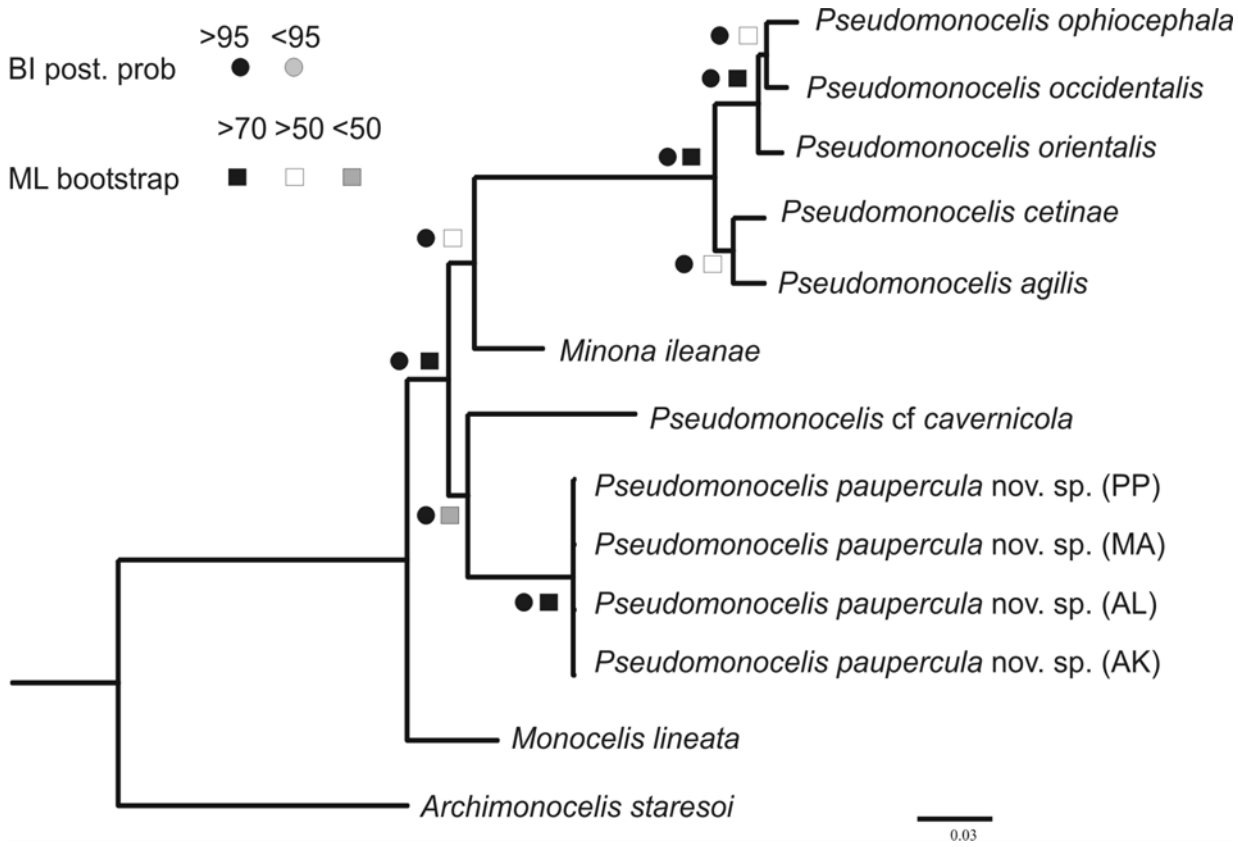

FIGURE 3. Tree obtained by BI showing the interrelationships of the species based on combined 18S+28S D1-D6. The branch length scale refers to the number of substitutions per site. Supports of main nodes are indicated for both BI (posterior probability) and ML (bootstrap) as a percentage.

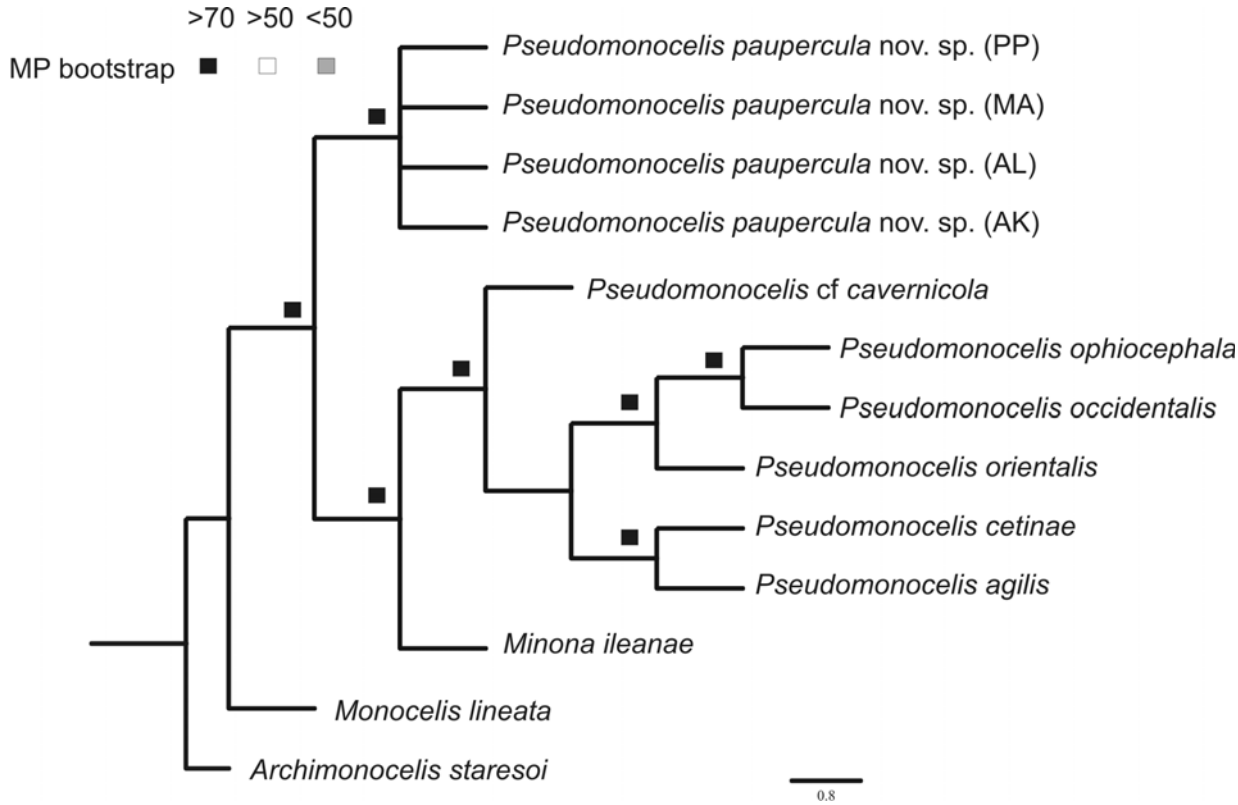

FIGURE 4. Tree obtained by MP showing the interrelationships of the species based on combined 18S+28S D1-D6. The branch length scale refers to the number of substitutions per site. Bootstrap nodal support is indicated as a percentage.

BI and ML were consistent in showing trees with the same topology, thus we reported the Bayesian trees only in Fig. 3. Both analyses do not resolve the genus *Pseudomononocelis* as monophyletic, since *M. ileanae* nests within it. *Pseudomonocelis paupercula* **nov. sp.** and *P.* cf *cavernicola* form a distinct clade (although not highly supported by both posterior probability and bootstrap values).

In the MP tree (Fig. 4), the new species of *Pseudomonocelis* is set as sister taxon of the remaining *Pseudomonocelis* species. Similarly to what is evidenced by BI and ML trees (Fig.3), *M. ileanae* is nested within the genus *Pseudomonocelis*. All nodes of the MP tree are highly supported.

Discussion

Species justification. Populations of *Pseudomonocelis paupercula* **nov. sp.** do not differ noticeably either in morphology and karyology (Table 2) across the range, which encompasses most of the Mediterranean. The new species is clearly distinct from congenerics, as it is the only species in the genus with a copulatory organ provided with a stylet. Its accessory organ is similar in position, size and, at least in part, morphology with that of *P. cavernicola.* However, in the latter species a glandular function has been excluded (Schockaert & Martens, 1987). Furthermore, *P. cavernicola* has a large bursa, provided with a vagina (Schockaert & Martens, 1987). The new species has the smallest haploid genome length (7.1-7.5 µm) known for the genus *Pseudomonocelis.* In the other species, genome length ranges from 9.1 µm (*Pseudomonocelis hoplites*) to 15.5 µm (*Pseudomonocelis caribbea* Curini-Galletti & Casu, 2005) (Curini-Galletti, 1997; Curini-Galletti & Casu, 2005). Sequences from *P. paupercula* **nov. sp.** form a highly supported and well separated cluster, meriting the designation of a new species.

Phylogenetic relationships. Our molecular sample, although limited, included species of the genus *Pseudomonocelis*, with postpharyngeal ovary, and species with prepharyngeal ovary (*Monocelis lineata*, *Minona ileanae*, and *Archimonocelis staresoi*). One of these species, *Minona ileanae*, is provided with an accessory (prostatoid) organ, with a stylet. This feature was given particularly relevant phylogenetic weight, and was used to split the Monocelididae into two subfamilies, based on the presence (Minoninae) or absence (Monocelidinae) of the organ (Karling, 1966). Later, Litvaitis *et al.* (1996), based on molecular, morphological and karyological data, considered the presence of the accessory organ as the plesiomorphic feature for the Monocelididae. Present systematic arrangement of the Monocelididae is mainly based on the morphology of the copulatory bulb, of the simplex-type in the Monocelidinae and of the duplex-type in the Duplomonocelidinae (Litvaitis *et al.*, 1996). However, the presence/absence of the accessory organ is still used to support the validity of otherwise morphologically identical genera, such as *Minona* and *Monocelis* in the Monocelidinae, and *Duplominona* Karling, 1966 and *Archilina* Ax, 1959 in the Duplomonocelidinae, respectively with and without this feature (Litvaitis *et al.*, 1996; Curini-Galletti *et al.*, 2010).

Results of the combined 18S + 28S D1-D6 analysis are conflictual with current, morphology-based definition of genera. In fact, the nesting of *M. ileanae* within *Pseudomonocelis* species shown by BI, ML and MP does not support the monophyly of the genus *Pseudomonocelis* (Figs 3-4).. Furthermore, this placement of *M. ileanae* is particularly difficult to justify on morphological grounds. Not only would it, in fact, require repeated losses of the accessory organ or of its stylet, but the most parsimonious explanation of the prepharyngeal position of the ovary in *M. ileanae* would then be that a reversal of the backward migration of the ovary has occurred in this species, further jeopardising present tenets in the taxonomy of the group. Interestingly, BI and ML trees (Fig. 3) suggest a sister-species relationships between *P.*cf *cavernicola* and *P. paupercula* **nov. sp.**. This would give further strength to the hypothesis that the presence of the accessory, muscular organ without stylet close to the female pore is a synapomorphic feature for the two species. However, this solution is poorly supported and the position of *P.* cf *cavernicola* is not consistent between BI and ML trees and the MP tree (Fig. 4). Thus, the limited sampling and the risks of parallelism in the group do not justify further (phylogenetic and biogeographical) considerations.

Conclusions

The present study highlights the problems of genera delimitation in a taxon such as the Monocelidinae, with comparatively very few morphological diagnostic characters, and where combination of character states may arise by parallel evolution. Given the conflicting results shown by the trees constructed on the combined 18S and 28S D1-D6 dataset, the need of a more extensive molecular and taxonomic sampling is apparent. On the other hand, this

research provides further evidence on the usefulness of rRNA fragments as markers for the molecular taxonomy of the Monocelidinae in which group the universal primers of the Cytochrome c Oxidase subunit 1 (the so-called Folmer region) often fail to produce adequate sequences (see e.g. Sanna *et al.*, 2009).

Finally, it is worth mentioning that *Pseudomonocelis paupercula* **nov. sp.** has been only very rarely encountered during samplings in the Mediterranean and, even in the stations where it has been found, was strictly confined to sectors characterised by the presence of fresh-water outlets and mixed, silty sediment. Given the threats that coastal fresh-water habitats are facing in the Mediterranean, the species appears potentially vulnerable.

References

Casu, M., Lai, T., Sanna, D., Cossu, P. & Curini-Galletti M. (2009) An integrative approach to the taxonomy of the pigmented European *Pseudomonocelis* Meixner, 1943 (Platyhelminthes: Proseriata). *Biological Journal of Linnean Society*, 98, 907–922.

Casu, M., Sanna, D., Cossu, P., Lai, T., Francalacci, P. & Curini-Galletti M. (2011) Molecular phylogeography of the microturbellarian *Monocelis lineata* (Platyhelminthes: Proseriata) in the North-East Atlantic. *Biological Journal of the Linnean Society*, 103, 117–135.

Curini-Galletti, M. (1997) Contribution to the knowledge of the Proseriata (Platyhelminthes, Seriata) from eastern Australia: genera *Necia* Marcus, 1950 and *Pseudomonocelis* Meixner, 1938 (partim). *Italian Journal of Zoology*, 64, 75–81.

Curini-Galletti, M. & Casu, M. (2005) Contribution to the knowledge of the genus *Pseudomonocelis* Meixner, 1943 (Rhabditophora: Proseriata). *Journal of Natural History*, 39, 2187–2201.

Curini-Galletti, M., Casu, M. & Lai, T. (2011) On the *Pseudomonocelis agilis* (Schultze, 1851) complex (Platyhelminthes: Proseriata), with description of two new species. *Meiofauna marina*, in press.

Curini-Galletti, M., Martens, P.M. & Puccinelli, I. (1985) Karyological observations on Monocelididae (Turbellaria, Proseriata): Karyometrical analysis of four species pertaining to the subfamily Minoninae. *Caryologia*, 38, 67–75.

Curini-Galletti, M., Webster, B. L., Huyse, T., Casu, M., Schockaert, E.R., Artois, T & Littlewood, T. J. (2010) New insights on the phylogenetic relationships of the Proseriata (Platyhelminthes), with proposal of a new genus of the family Coelogynoporidae. *Zootaxa*, 2537, 1–18.

Gelman, A., Carlin, J.B., Stern, H.S. & Rubin, D.B. (1995) *Bayesian Data Analysis*. Chapman & Hall, London.

Hall, T.A. (1999) BioEdit: a user-friendly biological sequence alignment editor and analysis program for Windows 95/98/NT. *Nucleic Acids Symposium Series*, 41, 95–98.

Huelsenbeck, J.P. & Ronquist, F. (2001) MRBAYES: Bayesian inference of phylogenetic trees. *Bioinformatics*, 17, 754–755.

Karling, T.G. (1966) Marine Turbellaria from the Pacific Coast of North America IV. Coelogynoporidae and Monocelididae. *Arkiv för Zoologi*, 18, 493–528.

Lai, T., Curini-Galletti, M. & Casu, M. (2008) Genetic differentiation among populations of *Minona ileanae* (Platyhelminthes: Proseriata) from the Red Sea and the Suez Canal. *Journal of Experimental Marine Biology and Ecology*, 362, 9–17

Levan, A., Fredga, K. & Sandberg, AA. (1964) Nomenclature for centrometric position on chromosomes. *Hereditas*, 52, 201–220.

Littlewood, D.T.J., Curini-Galletti, M. & Herniou, E.A. (2000) The interrelationships of Proseriata (Platyhelminthes: Seriata) tested with molecules and morphology. *Molecular Phylogenetics and Evolution*, 16, 449–466.

Litvaitis, M.K., Curini-Galletti, M., Martens, P.M. & Kocher, T.D. (1996) A reappraisal of the systematics of the Monocelididae (Platyhelminthes, Proseriata) – Inferences for rDNA sequences. *Molecular Phylogenetics and Evolution*, 6, 150–156.

Martens, P. M. (1983) Three new species of Minoninae (Turbellaria, Proseriata, Monocelididae) from the North Sea, with remarks on the taxonomy of the subfamily. *Zoologica Scripta*, 12, 153–160.

Martens, P.M. (1984) Comparison of three different extraction methods for Turbellaria. *Marine Ecology Progress Series*, 14, 229–234.

Matthey, R. (1949) *Les chromosomes des Vertèbrès*. Rouge, Lausanne, 344 pp.

Posada, D. (2008) jModelTest: Phylogenetic Model Averaging. *Molecular Biology and Evolution*, 25, 1253–1256.

Ronquist, F. & Huelsenbeck, J.P. (2003) mrbayes 3: Bayesian phylogenetic inference under mixed models. *Bioinformatics*, 19, 1572–1574.

Sanna, D., Lai, T., Francalacci, P., Curini-Galletti, M. & Casu, M. (2009) Population structure of the *Monocelis lineata* (Proseriata, Monocelididae) species complex assessed by phylogenetic analysis of the mitochondrial Cytochrome c Oxidase subunit I (COI) gene. *Genetics and Molecular Biology*, 32, 864–867.

Schockaert, E.R. & Martens, P.M. (1987) Turbellaria from Somalia. IV. The genus Pseudomonocelis Meixner, 1943. *Monitore Zoologico Italiano*, 9, 101–115.

Swofford, D.L. (2003) PAUP*. Phylogenetic Analysis Using Parsimony (*and Other Methods), Version 4. Sinauer Associates, Sunderland, Massachusetts.

Thompson, J.D., Higgins, D.G. & Gibson, T.J. (1994) CLUSTAL W: improving the sensitivity of progressive multiple sequence alignment through sequence weighting, position-specific gap penalties and weight matrix choice. *Nucleic Acids Research*, 22:4673–4680.

Zwickl, D. J. (2006) Genetic algorithm approaches for the phylogenetic analysis of large biological sequence datasets under the maximum likelihood criterion. Ph.D. dissertation, The University of Texas at Austin. URL: www.bio.utexas.edu/faculty/antisense/garli/Garli.html.